

Rational Control of Viscoelastic Properties in Multicomponent Associative Polymer Networks

David M. Loveless, Sung Lan Jeon, and Stephen L. Craig*

Department of Chemistry and Center for Biologically Inspired Materials and Material Systems, P.M. Gross Chemical Laboratory, Duke University, Durham, North Carolina 27708-0346

Received August 24, 2005

ABSTRACT: We report here the formation and dynamic mechanical properties of metallo-supramolecular networks formed by mixtures of bis-Pd(II) and Pt(II) cross-linkers with poly(4-vinylpyridine) in DMSO. Precise control over the dynamic mechanical properties of the bulk materials is achieved through the dissociation kinetics of the metal–ligand coordination bond responsible for cross-linking, the density of the cross-links, and the relative amounts of multiple cross-links. In networks formed from multiple types of cross-linkers, discrete contributions from each type of cross-linker are evident in the bulk mechanical properties, rather than an average of the contributing species. The heterogeneous rheology is consistent with simple models, to the extent that complex viscoelastic responses can be rationally engineered.

Introduction

The use of highly specific intermolecular interactions has propagated through the fields of polymer and material science in recent years. The contributions of these interactions to polymer properties are greatest when the presence of the interactions creates entanglements between macromolecules that would not otherwise be present. Examples include linear supramolecular polymers (SP's),^{1–21} in which specific, reversible interactions define the main chain of a linear polymeric assembly, and SP networks, in which the reversible interactions create transient cross-links between covalent polymer constituents. Within SP networks, a wide variety of motifs have been employed as cross-linking agents,^{22–35} including noncovalent interactions such as hydrogen bonding and salt bridges and metallo-supramolecular interactions based on metal–ligand coordination. Recent metallo-supramolecular networks include Beck and Rowan's multiply responsive lanthanide-based networks,²² the cross-linked "universal polymer backbones" implemented by Pollino et al.,²³ and Vermonden et al.'s modular, neodymium-based coordination system.²⁴ The use of highly specific intermolecular interactions within SP's potentially provides access to a range of materials end points, if the underlying relationships between molecular and bulk material properties were fully understood and exploited. In particular, a central question in the rational design of SP's is the extent to which the properties of the isolated reversible interactions are relevant to those of a polymeric superstructure—does an understanding of the small molecule components facilitate the prediction of SP properties?

We have recently explored molecular mechanisms underlying the mechanical properties of both linear SP's^{36–40} and SP networks.^{41,42} The SP networks were formed via specific metal–ligand coordination between bis-Pd(II) and Pt(II) organometallic cross-linkers and poly(4-vinylpyridine), PVP, in DMSO. The association thermodynamics of the cross-linking interaction within either pair of Pd(II) complexes or Pt(II) complexes, and

therefore the equilibrium structures of the networks, are effectively identical, but the lifetimes of the cross-links vary from ~1 ms to tens of minutes. The steady shear viscosity and frequency-dependent dynamic mechanical moduli of the bulk materials were found to be related quantitatively to the pyridine exchange rates measured on model Pd(II) and Pt(II) complexes.^{41,42} Ligand exchange proceeds through a solvent-assisted pathway in both the model complexes and the networks, and so the bulk mechanical properties are determined by relaxations that occur when the cross-links are dissociated from the polymer backbone. It is how often the cross-links dissociate, however, rather than how long they remain dissociated, that determines the bulk mechanical properties.⁴² The excellent agreement seen in scaling relationships based on model compounds offers promise for the rational, molecular design of materials with tailored mechanical properties.

In this paper, we investigate further the relationship between the dynamics of small molecule interactions and those of bulk materials, extending our study to associating networks formed by multicomponent mixtures of cross-linkers. The bifunctional Pd(II) and Pt(II) compounds **1a–1d** (Figure 1) are similar in structure to those employed previously to cross-link PVP, but their synthesis is sufficiently scalable to permit a wide range of bulk studies. The thermodynamic and kinetic parameters of the metal–pyridine interactions are known for model complexes, and the rheological properties of the bulk materials are readily attributed to the dynamics of the molecular interactions. Networks formed from the addition of a single type of cross-linker behave similarly to those reported previously, but we report for the first time SP networks formed from mixtures of multiple cross-linkers with PVP. The resulting materials show highly predictable and tunable viscoelastic properties. The bulk rheology, including the dependence of the viscosity, the storage modulus plateau, and the lifetime of the network on the total and relative concentration of cross-linkers, is then interpreted successfully in the context of common transient network models. In SP networks formed from multiple types of cross-linkers, discrete contributions from each type of cross-linker are evident in the bulk mechanical proper-

* Corresponding author. E-mail: stephen.craig@duke.edu.

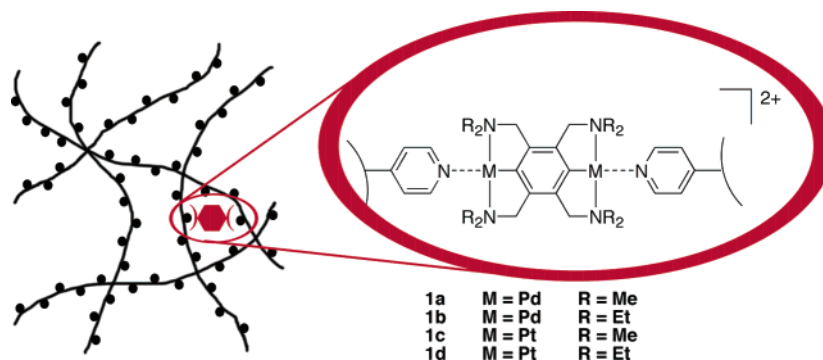


Figure 1. Schematic picture of networks formed from PVP chains and cross-linking bimetallic compounds (**1a–d**). Charges and counterions not shown for clarity.

ties, rather than an average of the contributing species. The independent control of diverse but highly specific cross-link dynamics is shown to provide a mechanism for the rational molecular engineering of complex viscoelastic behaviors in bulk materials.

Experimental Section

Materials. Dimethyl sulfoxide (DMSO) and poly(4-vinylpyridine) (PVP), $M_w = 60\,000$, were used as received from Aldrich. Compounds **1a–d** were synthesized as reported elsewhere.⁴³

Sample Preparation. Networks were formed as follows. To 1.1 g of DMSO was added 0.200 g of PVP. Cross-linking agent(s) **1a–d** were then added as solids to the vial, and enough DMSO was added to give a final sample that was 10% by total weight in PVP and cross-linker(s). The sample was then annealed three times at 80 °C.

Rheology. All rheological data were obtained using a Bohlin VOR rheometer with a concentric cylinder geometry (fixed bob and rotating cup). The inner cylinder diameter was 25 mm with an outer cylinder diameter of 26 mm, a bob height of 21.4 mm, and a cone angle of 2.3°. The sample (~2 mL) was loaded into the cup, with heating when necessary to allow the material to flow into the geometry, and the bob was lowered into the cup. The sample was allowed to equilibrate to 20 °C. Low deformation oscillatory data were obtained and processed with Bohlin VOR software. Torque bars (98.72, 10.42, and 0.245 g cm) were chosen so that the recorded stress moduli were within 10–90% of the dynamic range of the detector.

Results

Single-Component Cross-Linkers. Mixtures of PVP and bis-functional metal compounds **1a–1d** (Figure 1) formed faint yellow sols or gels at 10 wt % in DMSO. At these concentrations, solutions of PVP alone do not appear to be entangled. Similar mixtures of PVP with analogous monofunctional metal complexes are free-flowing,⁴¹ and the change in viscosity is attributed to reversible cross-linking of the PVP by **1** to form a network shown schematically in Figure 1. Four separate networks, each 10 wt % in DMSO and consisting of 5% (by metal functional group per pyridine residue) of a different cross-linker **1**, were created in DMSO. The thermodynamics and kinetics of the metal–pyridine interactions have been explored previously,^{41,42} and the equilibrium association constants K_{eq} and pyridine dissociation rate constants k_d are summarized for convenience in Table 1. Given the high concentrations of pyridine residues (~1 M), nearly all (>97–99%) of the metal centers are expected to be bound to the PVP, and so the structure of the networks (distribution and number of cross-links) is effectively constant across the

series. Previous studies demonstrated that the fundamental differences in mechanics among a similar series of four networks are directly attributed to the rates k_d at which pyridine dissociates from the metal center.^{41,42}

Table 1. Equilibrium Constants and Dissociation Rate Constants for Pincer Pd and Pt Complexes **1 with Pyridine (**2**) in DMSO at 25 °C [Uncertainties: K_{eq} ($\pm 20\%$), k_d ($\pm 15\%$)]**

complex	K_{eq} (M^{-1})	k_d (s^{-1})
1a·2	29 ^a	1450 ^b
1b·2	33 ^a	17 ^b
1c·2	8000 ^a	0.026 ^a
1d·2	4000 ^a	0.0006 ^a

^a Reference 41. ^b Reference 42.

To first characterize these new, single-component cross-linked systems, low-deformation oscillatory rheological studies were performed across a range of frequencies. In all four cases, the properties of “weak”⁴⁴ gels are observed. The dynamic viscosities of the networks as a function of oscillatory frequency are shown in Figure 2. As reported previously for a related network, the dynamic viscosities of the four systems differ significantly from one another: the low-frequency plateau $\eta_{\omega \rightarrow 0}$ is inversely proportional to the ligand dissociation rate k_d measured on model compounds, and the threshold frequency ω at which a decrease in η becomes noticeable is higher for high k_d (Figure 2a). That these shifts in all four cases are quantitatively determined by the kinetics of ligand exchange is shown in the scaled fits of Figure 2b. When the viscosity is scaled by the ligand dissociation rate k_d , taken from previous studies of model systems, and the frequency of the applied strain is scaled inversely by the same value, the raw dynamic viscosity data of Figure 2a collapse onto the master plot shown in Figure 2b. Similar agreement is seen for the storage modulus G' as a function of scaled frequency of the applied strain (Figure 3).

Classical transient network theories^{45–48} predict that the dynamic moduli (G' and G'') of self-associating networks follow the Maxwellian models shown in eqs 1 and 2. In these equations, G_0 is the plateau of the storage modulus and β is the relaxation rate of the network:

$$G' = G_0(\omega/\beta)^2/(1 + (\omega/\beta)^2) \quad (1)$$

$$G'' = G_0(\omega/\beta)/(1 + (\omega/\beta)^2) \quad (2)$$

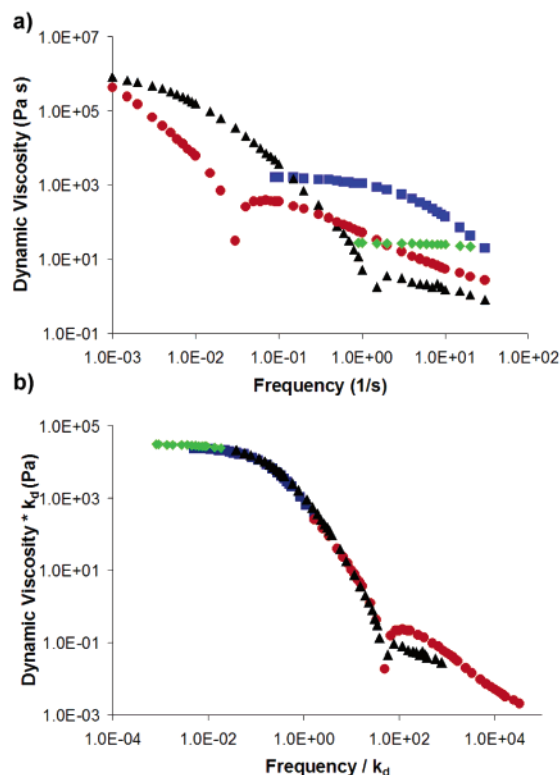


Figure 2. (a) Dynamic viscosity vs frequency for the networks 1-PVP and (b) the same dynamic viscosity scaled by k_d of the metal–pyridine bond of the cross-linker vs the frequency of oscillation scaled by k_d . Each of the networks consists of 5% (by metal functional group per pyridine residue) of (♦) **1a**, (■) **1b**, (▲) **1c**, and (●) **1d** and PVP at 10% by total weight of network in DMSO at 20 °C.

A comparison of the experimental data for 5% **1c**-PVP and the best fit of eqs 1 and 2 is shown in Figure 4, with $G_0 = 25$ kPa and $\beta = 0.00833$ s⁻¹. The fits are typically poor; the G' data deviate from the Maxwellian model at lower frequencies, and G'' deviates at higher frequencies. For $\omega < \beta$, the Maxwell model predicts that G' will scale as $\omega^{2.0}$, while the observed scaling law is $\omega^{0.8}$ across the data range shown in Figure 4a. Cates has noted that deviations from ideal Maxwell behavior are commonly observed in transient networks,⁴⁹ and they appear to be general for the systems at hand. Tanaka and Edwards have reported that deviations from the Maxwell model may arise from heterogeneity in the distribution of cross-linkers along the polymer chains, an explanation that is consistent with the observation that the deviation from the Maxwell model also scales with the same, single molecular dissociation rate.⁴⁸

Multicomponent Cross-Linkers. A network consisting of PVP with two cross-linkers—**1a** and **1c** at a cross-linking concentration of 2.5% (by functional group equivalent relative to pyridine) of each—was formed at 10 wt % in DMSO. Hereafter, we use the symbol N_{ac} to refer to this network formed from an equimolar mixture of components **1a** and **1c**, and throughout the remainder of the paper, that nomenclature is applied generally to networks with mixtures of cross-linkers. The network N_{ac} has the same equilibrium cross-linking structure as the single-component networks characterized above, but now the cross-link dynamics that govern mechanical properties are heterogeneous at the molecular level.

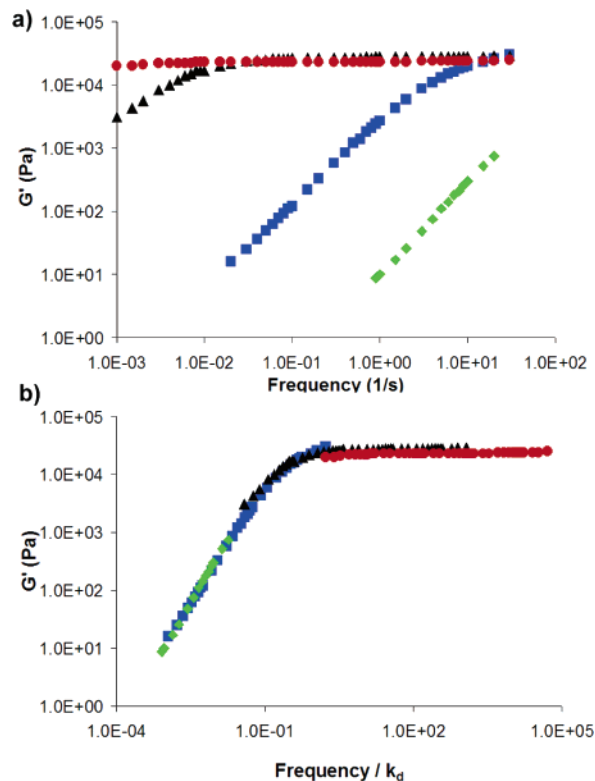


Figure 3. (a) Storage modulus G' for the networks 1-PVP and (b) the same storage modulus vs the frequency of oscillation scaled by k_d . Each of the networks consists of 5% (by metal functional group per pyridine residue) of (♦) **1a**, (■) **1b**, (▲) **1c**, and (●) **1d** and PVP at 10% by total weight of network in DMSO at 20 °C.

To test the effect of that heterogeneity, the dynamic viscosity and storage modulus G' were monitored as a function of frequency, as shown in Figures 5 and 6. The behavior of N_{ac} was compared to networks made of PVP with 5% of either **1a** or **1c** or 2.5% of either **1a** or **1c**, all at the same concentration of 10% by total weight in DMSO. Below $\omega = 1$ s⁻¹, the dynamic viscosity of N_{ac} closely mimics that of the network consisting entirely of the slower component **1c**-PVP at a concentration of 2.5% (Figure 5). As ω increases to values greater than 1 s⁻¹, the dynamic viscosity of N_{ac} becomes nearly constant with increasing frequency (up to the limit of the rheometer) and effectively behaves like a network comprising PVP and 5% of the faster cross-linking component **1a**.

Similar effects are observed in the storage modulus G' (Figure 6). At low frequencies, the spectrum resembles that of the 2.5% **1c**-PVP network, achieving a plateau of about 3 kPa from $\omega = 0.02$ – 10 s⁻¹. Above 10 s⁻¹, there appears to be a slight upturn in G' as the storage modulus begins to take on some of the character of the 5% **1a**-PVP network.

A second network with multicomponent cross-linking, N_{bc} , was formed from a mixture of PVP with 2.5% each of **1b** and **1c**, still at 10 wt % in DMSO. The dynamic viscosity and storage modulus of N_{bc} were compared to networks made of PVP with 5% of either **1b** or **1c**, or 2.5% of either **1b** or **1c**, again at the same 10% concentration in DMSO (Figures 7 and 8). Very similarly to N_{ac} , the dual cross-linker network N_{bc} exhibits characteristics of each of the two distinct single-component networks. Below a critical frequency of 0.03

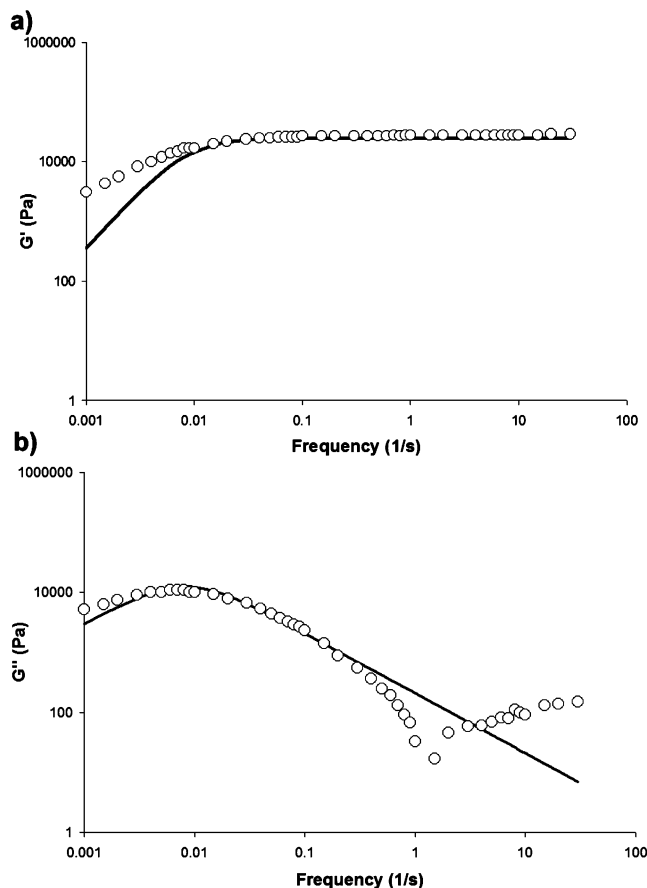


Figure 4. Dynamic moduli (open circles) of a 5% **1c**-PVP network at 10 wt % in DMSO, 20 °C, and the corresponding Maxwellian fits (solid lines) based on eqs 1 and 2 for (a) G' and (b) G'' , respectively.

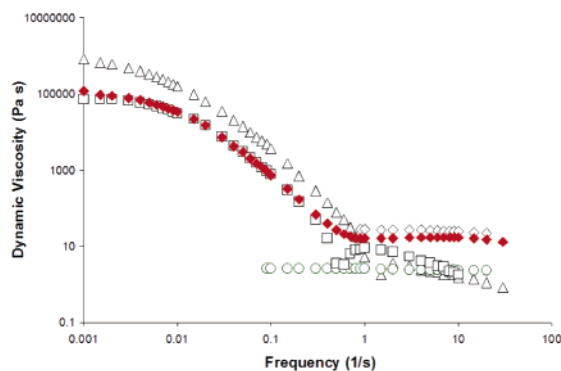


Figure 5. Dynamic viscosity vs frequency for networks (◆) N_{ac} , (□) 2.5% **1c**-PVP, (△) 5% **1c**-PVP, (○) 2.5% **1a**-PVP, and (◇) 5% **1a**-PVP. All networks at 10% by total weight in DMSO, 20 °C.

s^{-1} , both the viscosity (Figure 7) and storage modulus (Figure 8) are nearly identical to that of the network comprising exclusively PVP and 2.5% of the slower component **1c**. When the frequency of applied oscillatory strain approaches the point that the dynamic viscosity of a 5% **1b**-PVP network is comparable to the dynamic viscosity of the 2.5% **1c**-PVP network, a transition occurs, and N_{bc} behaves like the 5% **1b**-PVP network above that frequency. Similar behavior is observed in the G' data of Figure 8; the storage modulus traces the 2.5% **1c**-PVP data at low frequencies before a transition to 5% **1b**-PVP data at higher frequencies (although we

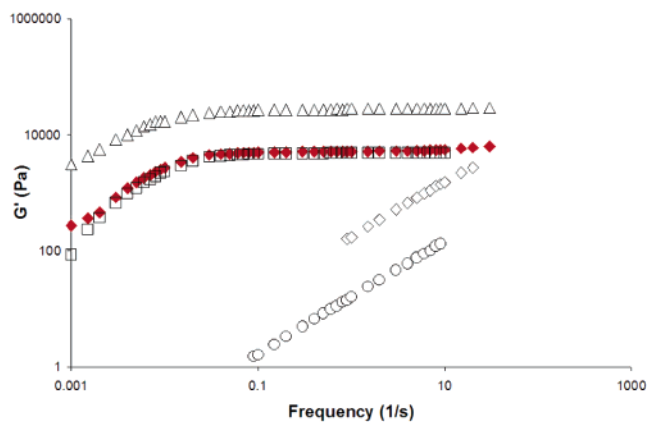


Figure 6. Storage modulus, G' , vs frequency for networks (◆) N_{ac} , (□) 2.5% **1c**-PVP, (△) 5% **1c**-PVP, (○) 2.5% **1a**-PVP, and (◇) 5% **1a**-PVP. All networks at 10% by total weight in DMSO, 20 °C.

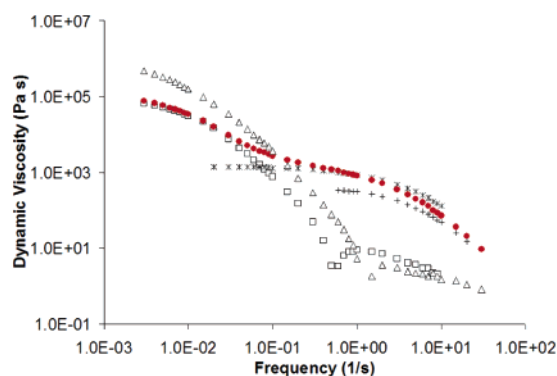


Figure 7. Dynamic viscosity vs frequency for networks (●) N_{bc} , (□) 2.5% **1c**-PVP, (△) 5% **1c**-PVP, (+) 2.5% **1b**-PVP, and (*) 5% **1b**-PVP. All networks 10% by total weight in DMSO, 20 °C.

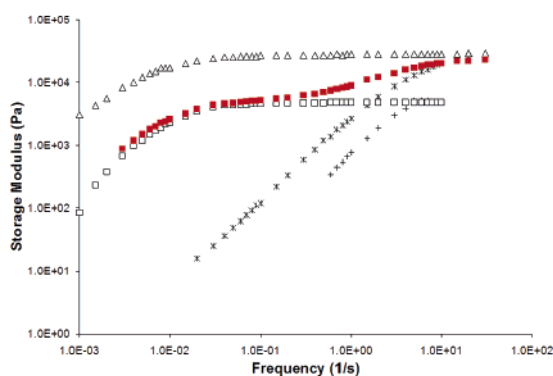


Figure 8. Storage modulus, G' , vs frequency for (■) N_{bc} , (□) 2.5% **1c**-PVP, (△) 5% **1c**-PVP, (+) 2.5% **1b**-PVP, and (*) 5% **1b**-PVP. All networks 10% by total weight in DMSO, 20 °C.

point out that all 5% single-component networks plateau at the same value of $G_0 = 2.8 \times 10^4$ Pa).

A final network featuring multicomponent cross-linking was formed from three cross-linkers. The network N_{abc} contains PVP with 1.66% each of **1a**, **1b**, and **1c** at a total concentration of 10 wt % in DMSO. The dynamic mechanical properties of N_{abc} exhibit more complexity than (but the same trends) seen in the two-component cross-linking networks N_{ac} and N_{bc} (Figure 9). The dynamic mechanical properties of N_{abc} are similar to those of a 1.66% network of **1c**-PVP at low

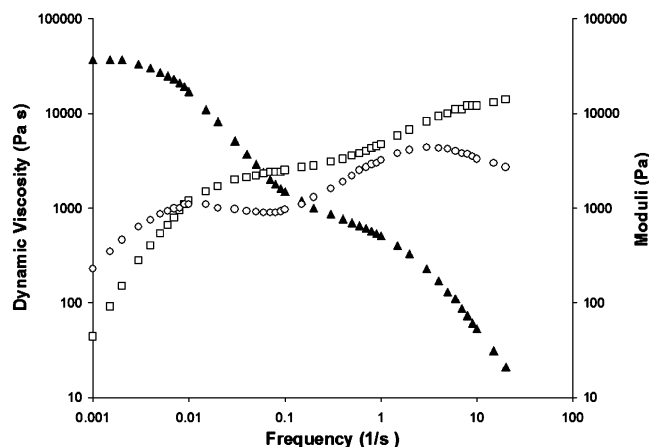


Figure 9. (▲) Dynamic viscosity and moduli, (□) G' and (○) G'' , vs frequency for N_{abc} , 10% by total weight in DMSO, 20 °C.

frequencies and a 3.33% network of **1b**•PVP at intermediate frequencies, and there is an apparent shift toward those of a 5% network of **1a**•PVP at high frequencies.

Discussion

Single-Component Cross-Linking. The single-component cross-linked networks of **1**•PVP display behavior that is quantitatively similar to that observed in our previous studies of a similar system.^{41,42} The networks reported here are slightly more viscous than those examined in the earlier work, a difference we attribute primarily to the higher total concentration in the present study (10 vs 8.3 wt %). Nonetheless, the underlying molecular mechanisms of bulk mechanics are the same; it is the dynamics of cross-link dissociation, rather than the rate constant for association and the obviously related equilibrium association constant for cross-link formation, that determine the mechanical properties of the networks. The validity of the molecule-to-material relationship is driven home by Figures 2b and 3b, in which the disparate bulk data are convincingly scaled to a master curve through the pyridine ligand dissociation rates determined on model metal complexes. The scaling includes a change in behavior observed in the dynamic viscosity of the **1c**•PVP and **1d**•PVP networks at $\omega/k_d = \sim 60$. The precise nature of this transition is not known, but the conservation of the onset upon scaling indicates that its origins lie in the relative contribution of cross-link dissociation.

Transient network models motivate the use of the Maxwell equations to describe the data, and single-exponential fits (one value of β in eqs 1 and 2) provide reasonable agreement with the experimental data (Figure 4). In addition to the high-frequency transition in dynamic viscosity discussed in the preceding paragraph, however, deviation is also observed from the Maxwell fits to G' at frequencies lower than the bulk relaxation rate β . Likely explanations for this deviation include a distribution of cross-linker separations⁴⁸ and some cooperativity between multiple cross-linkers that leaves a greater-than-expected fraction of the cross-links intact at low frequencies. These deviations and further characteristics of single-component networks, however, are not immediately relevant to the present investigation and will be reported elsewhere.

Multicomponent Cross-Linking. The emphasis of the current work, instead, is on the effects of multicomponent cross-linking on the dynamic mechanical properties of the networks. Throughout the networks with multicomponent cross-linking constituents, it is the slow cross-links that control the mechanical properties of the network at low-frequency oscillations. For example, in both N_{bc} and N_{ac} , the slower platinum cross-linkers provide the dominant feature of the networks at $\omega \rightarrow 0$, as evidenced by dynamic viscosities that overlap that of a 2.5% **1c**•PVP network in both cases. The resistance to flow is determined by the slower cross-linkers; the faster components **1a** or **1b** dissociate and relax rapidly on the time scale of **1c** dissociation, and they are therefore “invisible” in their contributions to viscous relaxations. As the frequency of oscillation increases, however, the slower cross-links are now effectively “intact” on the time scale of the measurement, and the relaxations that dominate the viscous loss of the bulk network are those that involve the 2.5% of the faster components **1a** or **1b**. Importantly, the presence of the slower **1c** cross-linkers is still felt; the viscous loss in this regime more closely parallels that of 5% **1a** or **1b** (although the highest frequency data, $\omega > 10 \text{ s}^{-1}$, for N_{bc} is ambiguous). The slower cross-links, effectively intact at high frequency, apparently limit the extent of relaxation that can occur upon dissociation of the faster cross-linkers.

Similar behavior is observed in the elastic storage modulus data. At low frequencies, only a small fraction of the slower cross-linkers remains intact, and the storage modulus parallels that of the 2.5% **1c**•PVP network. The overlap continues into a plateau region, at which point essentially all of the **1c** cross-links remain intact and elastically store the applied strain. As the applied frequency increases toward the dissociation rate of the faster components (either **1a** or **1b**), the previously fluid fast components now remain largely intact, and the storage modulus again increases toward a second plateau. In the case of N_{bc} , that plateau is experimentally obtainable, and it overlaps at the same G_0 of 28 kPa found in each of the single-cross-linker 5% networks. We note that, as observed in the dynamic viscosity data, the contributions of each of the two cross-linking components are influenced by the other component. The observed G_0 of 28 kPa is that of a 5% cross-linked network; it is not the sum of the moduli of two networks with 2.5% cross-linking equivalents ($\sim 3 \text{ kPa}$ each).

The observed behavior, as described above, is essentially that of transient network models, in which the independent relaxations of stress-bearing entanglements determines the dynamic mechanical response of a network. More sophisticated, quantitative transient network models of networks with multiple types of cross-linkers have been developed previously by Jongschaap and co-workers.⁵⁰ Those authors explicitly account for the interconnections between segments that are joined by multiple types of cross-linkers. Their model predicts multiple plateaus in G' that are similar to those observed here. Direct comparisons with the previous theoretical results are complicated, however, because either the fraction of intact cross-linkers (through the equilibrium constant) or molecular weight of the polymer main chain is typically varied in the theoretical work, while those variables are kept effectively constant here.

Although neither the exact structure of the networks, detailed mechanism of relaxation,^{48,50–52} nor the extent of cooperativity in the associations is known precisely from the present analysis, individual dissociation events clearly dominate the bulk properties. The contributions of the individual components are evident within networks formed from multicomponent cross-linkers; no significant averaging or summation of different components is observed. Given the structural homology among the cross-linkers **1** and the effectively identical behavior of the scaled dynamic mechanical response in Figures 2b and 3b, segregation of different cross-linking components is extremely unlikely. Within a randomly dispersed network, therefore, these results strongly support earlier conclusions that the cross-linkers act as independent entanglement points whose dynamics are not affected dramatically by the presence of additional cross-linkers.^{41,42}

The independence of the cross-linkers has significant consequences for the rational, molecular engineering of bulk viscoelastic properties. As in the case at hand, when entanglements are defined by very specific interactions, the chemical control of bulk properties follows. As long as the strength of the association is great enough to render associated a significant fraction of the cross-linkers, the dynamics of cross-link dissociation, rather than further details of their thermodynamics, are the key design criterion, and quite complex viscoelastic behavior can be engineered given suitable knowledge of the small molecules. A hint of the potential of such an approach is seen in the dynamic mechanical properties of the tricomponent network N_{abc} (Figure 9). Multiple transitions in both storage and loss moduli are clearly seen, and the location and magnitude of those transitions are clearly determined by the dissociation dynamics and relative concentrations of the three cross-linkers. While the N_{abc} example is somewhat artificial, its properties demonstrate that the behaviors observed in the two-component cross-linked networks may be successfully extrapolated to more complex networks.

More generally, the results presented here speak to the potential of reversible and specific intermolecular interactions as effectors of the entanglements or polymer bridges^{38,39,53} necessary to transmit force in materials. The sophistication available in the field of molecular recognition holds considerable promise as it is applied increasingly to areas of material science. Whether in cross-linked networks^{22–34} or linear supramolecular polymers,^{1–21} the thermodynamics of the intermolecular interaction are a primary design consideration, but the dynamics of the interaction are particularly important under nonequilibrium conditions such as those imposed by a mechanical stress. As shown here, the rational design and synthesis of materials with very specific and customized viscoelastic properties might be realized by exploiting an understanding of those dynamics.

Conclusions

We have reported the rational control of dynamic mechanical properties in multicomponent self-associating networks. The control is facilitated by the use of different Pd(II) and Pt(II) organometallic cross-linkers within a single poly(4-vinylpyridine)-based network, and the lifetimes of the coordinative cross-linkers range from milliseconds to tens of minutes. By controlling the dissociation rate of the transient cross-links, it is possible to control the dynamic viscosity and the elastic

storage modulus widely, precisely, and predictably. The mechanical properties directly reflect the dynamics of the individual cross-linking components, rather than an averaged, cooperative behavior of multiple cross-links.

Acknowledgment. This work was supported by NSF and NIH. D.M.L. is grateful for an NSF IGERT Fellowship (DGE-0221632) and Burroughs Wellcome Fellowship from the Duke University Department of Chemistry. S.L.C. gratefully acknowledges a DuPont Young Professor Award and a Camille and Henry Dreyfus New Faculty Award. We thank S. Zauscher for the use of his rheometer.

References and Notes

- (1) Lehn, J.-M. *Makromol. Chem., Macromol. Symp.* **1993**, 1–17.
- (2) Hilger, C.; Stadler, R. *Makromol. Chem.* **1991**, 805–817.
- (3) Sijbesma, R. P.; B., F. H.; Brunsveld, L.; Folmer, B. J. B.; Hirschberg, J. H. K. K.; Lange, R. F. M.; Lowe, J. K. L.; Meijer, E. W. *Science* **1997**, 278, 1601–1604.
- (4) Dankers, P. Y. W.; van Beek, D. J. M.; ten Cate, A. T.; Sijbesma, R. P.; Meijer, E. W. *Polym. Mater. Sci. Eng.* **2003**, 88, 52–53.
- (5) ten Cate, A. T.; van Beek, D. J. M.; Spiering, A. J. H.; Dankers, P. Y. W.; Sijbesma, R. P.; Meijer, E. W. *Polym. Prepr. (Am. Chem. Soc., Div. Polym. Chem.)* **2003**, 44, 618–619.
- (6) Hirschberg, J. H. K. K.; Ramzi, A.; Sijbesma, R. P.; Meijer, E. W. *Macromolecules* **2003**, 36, 1429–1432.
- (7) Sijbesma, R. P.; Folmer, B. J. B.; Meijer, E. W. *Polym. Prepr. (Am. Chem. Soc., Div. Polym. Chem.)* **2002**, 43, 375–376.
- (8) Bosman, A. W.; Folmer, B. J. B.; Hirschberg, J. H. K. K.; Keizer, H. M.; Sijbesma, R. P.; Meijer, E. W. *Polym. Prepr. (Am. Chem. Soc., Div. Polym. Chem.)* **2002**, 43, 322.
- (9) Castellano, R. K.; Rudkevich, D. M.; Rebek, J., Jr. *Proc. Natl. Acad. Sci. U.S.A.* **1997**, 94, 7132–7137.
- (10) Knapp, R.; Schott, A.; Rehahn, M. *Macromolecules* **1996**, 29, 478–480.
- (11) Meier, M. A. R.; Schubert, U. S. *Polym. Mater. Sci. Eng.* **2003**, 88, 193–444.
- (12) Hofmeier, H.; El-Ghayoury, A.; Schubert, U. S. *Polym. Prepr. (Am. Chem. Soc., Div. Polym. Chem.)* **2003**, 44, 709–710.
- (13) Hofmeier, H.; Gohy, J.-F.; Schubert, U. S. *Polym. Mater. Sci. Eng.* **2003**, 88, 193–194.
- (14) Hofmeier, H.; Schmatloch, S.; Schubert, U. S. *Polym. Prepr. (Am. Chem. Soc., Div. Polym. Chem.)* **2003**, 44, 711–712.
- (15) Schmatloch, S.; Gonzalez, M. F.; Schubert, U. S. *Macromol. Rapid Commun.* **2002**, 23, 957–961.
- (16) Gohy, J.-F.; Lohmeijer, B. G. G.; Varshney, S. K.; Decamps, B.; Leroy, E.; Boileau, S.; Schubert, U. S. *Macromolecules* **2002**, 35, 9748–9755.
- (17) Gohy, J.-F.; Lohmeijer, B. G. G.; Varshney, S. K.; Schubert, U. S. *Macromolecules* **2002**, 35, 7427–7435.
- (18) Lohmeijer, B. G. G.; Schubert, U. S. *Angew. Chem., Int. Ed.* **2002**, 41, 3825–3829.
- (19) Schubert, U. S.; Eschbaumer, C. *Angew. Chem., Int. Ed.* **2002**, 41, 2892–2926.
- (20) Schubert, U. S.; Schmatloch, S.; Precup, A. A. *Des. Monomers Polym.* **2002**, 5, 211–221.
- (21) Paulusse, J. M. J.; Huijbers, J. P. J.; Sijbesma, R. P. *Macromolecules* **2005**, 38, 6290–6298.
- (22) (a) Beck, J. B.; Rowan, S. J. *J. Am. Chem. Soc.* **2003**, 125, 13922–13923. (b) Zhao, Y.; Beck, J. B.; Rowan, S. J.; Jamieson, A. M. *Macromolecules* **2004**, 37, 3529–3531.
- (23) Pollino, J. M.; Nair, K. P.; Stubbs, L. P.; Adams, J.; Weck, M. *Tetrahedron* **2004**, 60, 7205–7215.
- (24) Vermonden, T.; van Steenbergen, M. J.; Besseling, N. A. M.; Marcelis, A. T. M.; Hennink, W. E.; Sudhölter, E. J. R.; Cohen Stuart, M. A. *J. Am. Chem. Soc.* **2004**, 126, 15802–15808.
- (25) Kato, T.; Kihara, H.; Kumar, U.; Uryu, T.; Fréchet, J. M. J. *Angew. Chem., Int. Ed. Engl.* **1994**, 33, 1644–1645.
- (26) Brunsveld, L.; Folmer, B. J. B.; Meijer, E. W. *MRS Bull.* **2000**, 25, 49–53.
- (27) Rieth, L. R.; Eaton, R. F.; Coates, G. W. *Angew. Chem., Int. Ed.* **2001**, 40, 2153–2156.
- (28) Zhao, Y.; Yuan, G.; Roche, P. *Polymer* **1999**, 40, 3025–3031.
- (29) Loontjens, T.; Put, J.; Coussens, B.; Lange, R.; Palmen, J.; Sleijpen, T.; Plum, B. *Makromol. Symp.* **2001**, 174, 357–371.

- (30) Hilger, C.; Dräger, M.; Stadler, R. *Macromolecules* **1992**, *25*, 2498–2501.
- (31) Müller, M.; Dardin, A.; Seidel, U.; Balsamo, V.; Iván, B.; Spiess, H. W.; Stadler, R. *Macromolecules* **1996**, *29*, 2577–2583.
- (32) Thilbault, R. J.; Hotchkiss, P. J.; Gray, M.; Rotello, V. M. *J. Am. Chem. Soc.* **2003**, *125*, 11249–11252.
- (33) Lange, R. F. M.; van Gurp, M.; Meijer, E. W. *J. Polym. Sci., Part A: Polym. Chem.* **1999**, *37*, 3657–3670.
- (34) Park, T.; Zimmerman, S. C.; Nakashima, S. *J. Am. Chem. Soc.* **2005**, *127*, 6520–6521.
- (35) McKee, M. G.; Elkins, C. L.; Park, T.; Long, T. E. *Macromolecules* **2005**, *38*, 6015–6023.
- (36) Xu, J.; Fogleman, E. A.; Craig, S. L. *Macromolecules* **2004**, *37*, 1863–1870.
- (37) Fogleman, E. A.; Yount, W. C.; Xu, J.; Craig, S. L. *Angew. Chem., Int. Ed.* **2002**, *41*, 4026–4028.
- (38) Kersey, F. R.; Lee, G.; Marszalek, P.; Craig, S. L. *J. Am. Chem. Soc.* **2004**, *126*, 3038–3039.
- (39) Kim, J.; Liu, Y.; Ahn, S. J.; Zauscher, S.; Karty, J. M.; Yamanaka, Y.; Craig, S. L. *Adv. Mater.* **2005**, *17*, 1749–1753.
- (40) Yount, W. C.; Juwarker, H.; Craig, S. L. *J. Am. Chem. Soc.* **2003**, *125*, 15302–15303.
- (41) Yount, W. C.; Loveless, D. M.; Craig, S. L. *Angew. Chem., Int. Ed.* **2005**, *44*, 2746–2748.
- (42) Yount, W. C.; Loveless, D. M.; Craig, S. L. *J. Am. Chem. Soc.* **2005**, *127*, 14488–14496.
- (43) Jeon, S. L.; Loveless, D. M.; Yount, W. C.; Craig, S. L. Manuscript in preparation.
- (44) van Esch, J.; Feringa, B. L. In *Encyclopedia of Supramolecular Chemistry*; Atwood, J. L., Steed, J. W., Eds.; M. Dekker: New York, 2004; Vol. 2, pp 586–594.
- (45) Green, M. S.; Tobolsky, A. V. *J. Chem. Phys.* **1946**, *14*, 80–89.
- (46) Lodge, A. S. *Trans. Faraday Soc.* **1956**, *52*, 120–130.
- (47) Shikata, T.; Hirata, H.; Takatori, E.; Osaki, K. *J. Non-Newtonian Fluid Mech.* **1988**, *28*, 171–182.
- (48) Tanaka, F.; Edwards, S. F. *Macromolecules* **1992**, *25*, 1516–1523.
- (49) Cates, M. E.; Candau, S. J. *J. Phys.: Condens. Matter* **1990**, *2*, 6869–6892.
- (50) Jongschaap, R. J. J.; Wientjes, R. H. W.; Duits, M. H. G.; Mellema, J. *Macromolecules* **2001**, 1031–1038.
- (51) Leibler, L.; Rubinstein, M.; Colby, R. H. *Macromolecules* **1991**, *24*, 4701–4707.
- (52) Semenov, A. N.; Rubinstein, M. *Macromolecules* **2002**, *35*, 4821–4837.
- (53) Zou, S.; Schonherr, H.; Vancso, G. J. *Angew. Chem., Int. Ed.* **2005**, *44*, 956–959.

MA0518611